

NUREG/CR-2281, Vol. 4

LA-9305-PR

Progress Report

Los Alamos National Laboratory is operated by the University of California for the United States Department of Energy under contract W-7405-ENG-36.

# *Nuclear Reactor Safety*

*October 1—December 31, 1981*

Los Alamos Los Alamos National Laboratory  
Los Alamos, New Mexico 87545

8208120368 820731  
PDR NUREG  
CR-2281 R PDR

An Affirmative Action/Equal Opportunity Employer

The four most recent reports in this series, unclassified, are NUREG/CR-2266, LA-8935-PR; NUREG/CR-2281, Vol. 1, LA-8945-PR; NUREG/CR-2281, Vol. 2, LA-9209-PR; and NUREG/CR-2881, Vol. 3, LA-9229-PR.

Edited by Nancy Sheheen, Q Division

NOTICE

This report was prepared as an account of work sponsored by an agency of the United States Government. Neither the United States Government nor any agency thereof, or any of their employees, makes any warranty, expressed or implied, or assumes any legal liability or responsibility for any third party's use, or the results of such use, of any information, apparatus, product or process disclosed in this report, or represents that its use by such third party would not infringe privately owned rights.

## Nuclear Reactor Safety

October 1—December 31, 1981

Compiled by  
Michael G. Stevenson

Manuscript submitted: March 1982  
Date published: May 1982

Prepared for  
Division of Accident Evaluation  
Office of Nuclear Regulatory Research  
US Nuclear Regulatory Commission  
Washington, DC 20555

NRC FIN Nos.		
A7014	A7027	A7212
A7015	A7049	A7228
A7016	A7053	A7235

NUCLEAR REACTOR SAFETY  
October 1 - December 31, 1981

Compiled by

Michael G. Stevenson

ABSTRACT

The work that is highlighted here represents accomplishments for the period October 1 - December 31, 1981 by the groups at Los Alamos involved in reactor safety research for the Division of Accident Evaluation, Office of Nuclear Regulatory Research of the US Nuclear Regulatory Commission. Presented are brief overviews compiled by project, along with a bibliography of Technical Notes and publications written during this quarter.



TRAC CODE DEVELOPMENT  
FIN A7016

TRAC-PF1 DEVELOPMENT (J. H. Mahaffy)

During the fourth quarter we completed the documentation for the Transient Reactor Analysis Code (TRAC)-PF1 and prepared for the TRAC-PF1 workshop, which was conducted on November 17-19. We have completed a draft of the code manual, and the editing process is under way. We also have completed a large part of the TRAC-PF1 developmental assessment manual and initiated the editing. Additionally, we have generated supplemental notes for the workshop participants.

Since the workshop, we have concentrated on the code improvements for TRAC-PF1/MOD1, scheduled for release by November 30, 1982. A detailed study of the code changes necessary to implement the improvements requested by the Nuclear Regulatory Commission indicated that substantial additions to the TRAC-PF1 steam-generator model are required. The turbine model has been developed to the point where FORTRAN coding could begin.

At the time of the workshop, Los Alamos changed the method of implementing changes in TRAC. Previously, a text editor available only through the Livermore Time-Sharing System (LTSS) incorporated changes in the code. The limited availability of this text editor made Los Alamos error corrections difficult to implement on other computer systems. We have switched TRAC maintenance and development at Los Alamos to the Control Data Corporation (CDC) Update, a standard utility for the majority of the external users and available to users with non-CDC equipment through a commercial software package. The CDC Update greatly simplifies code error corrections and modifications for the external users. However, the conversion to the CDC Update was inconsistent with the automated code maintenance utilities at Los Alamos, and a substantial effort is required to modify these utilities.

## THERMAL-HYDRAULIC ANALYSIS FOR REACTOR SAFETY RESEARCH

FIN A7027

### INTRODUCTION (B. J. Daly)

Research efforts during the past quarter were concentrated on three projects: the pressurized thermal shock study, the hydrogen migration study, and the Slab Core Test Facility (SCTF) upper-plenum de-entrainment study for the 2D/3D program. These investigations are all at the stage of model refinement, preparatory to engineering application. The pressurized-thermal-shock and hydrogen-migration studies require three-dimensional algorithms in their solutions.

### PRESSURIZED THERMAL SHOCK (B. J. Daly, F. H. Harlow, B. A. Kashiwa, and M. D. Torrey)

The SOLA-2D code<sup>1</sup> was modified extensively to analyze the mixing of vent valve and high-pressure injection (HPI) flows in the cold leg and downcomer for comparison with Creare experiments. The computational capability of the code was extended by the addition of an energy equation, an internal obstacle formulation, a variable mesh capability, an extended boundary condition treatment, a more complete input/output package, and a restart facility. Two-dimensional computations have been made in the planes of the cold leg and downcomer, and the results of these calculations have been compared with the Creare measurements. Progress also was made during this quarter in extending the SOLA-3D code<sup>2</sup> for application to the Creare studies and for the analysis of thermal mixing in the cold leg and downcomer of the Babcock and Wilcox Oconee reactor.

### HYDROGEN MIGRATION IN LIGHT-WATER REACTOR CONTAINMENTS (L. R. Stein and J. R. Travis)

The multidimensional fluid dynamics code K-FIX (Ref. 3) has been modified and extended to form a new code, HMS (Hydrogen Migration Studies),<sup>4</sup> for calculating the details of multispecies gas transport through containment structures. A two-dimensional version of the code, HMS(2D), can calculate the transport of air, hydrogen, and steam on a nonuniform grid in a Cartesian or axisymmetric coordinate system; and a three-dimensional version, HMS(3D), is under development. Both codes employ an interpolated-donor-cell convective scheme for improved accuracy.

HMS(2D) has been used to calculate the relative motion of air and hydrogen in multichambered regions for comparison with results of experiments performed at Battelle (Frankfurt).<sup>5</sup> These calculations show good agreement with the experimental measurements.

2D/3D WORK: DE-ENTRAINMENT IN THE SCTF UPPER PLENUM (B. J. Daly and F. H. Harlow)

Two-dimensional calculations were performed with the SAM code<sup>6</sup> to analyze upper-plenum de-entrainment relative to the SCTF experiments. A second liquid field was added to the code to represent liquid film motion on the control rod guide tubes and support columns, and a model was developed to account for mass exchange between the droplet field and this liquid film. This mass exchange model was based on droplet de-entrainment studies performed at Los Alamos and elsewhere.

At the present time we are refining the liquid film model for a more accurate accounting of liquid drainage from the upper-plenum structure and of pool formation at the upper-core support plate.

#### REFERENCES

1. C. W. Hirt, B. D. Nichols, and N. C. Romero, "SOLA - A Numerical Solution Algorithm for Transient Fluid Flows," Los Alamos Scientific Laboratory report LA-5852 (April 1975).
2. B. D. Nichols, C. W. Hirt, and L. R. Stein, "SOLA-3D: A Numerical Solution Algorithm for Transient 3D Flows," Los Alamos National Laboratory report (to be published).
3. W. C. Rivard and M. D. Torrey, "K-FIX: A Computer Program for Transient, Two-Dimensional, Two-Fluid Flow," Los Alamos Scientific Laboratory report LA-NUREG-6623 (April 1977).
4. J. R. Travis, L. R. Stein, M. D. Torrey, and F. H. Harlow, "HMS(2D): A Computer Program for Transient, Two-Dimensional, Hydrogen Migration Studies," Los Alamos National Laboratory report (to be published).
5. G. Langer, R. Jenior, and H. G. Wentlandt, "Experimentelle Untersuchung der Wasserstoffverteilung im Containment eines Leichtwasserreaktors nach einem Kuhlmitteilverlust-Storfall," Battelle Institut e.V. Frankfurt report BF-F-63.363-3 (1979). Also available as Nuclear Regulatory Commission Translation 801, "Experimental Investigation of the Hydrogen Distribution in the Containment of a Light-Water Reactor Following a Coolant Loss Accident" (1980).
6. B. J. Daly, A. A. Amsden, and F. H. Harlow, "SAM: A Computer Program for the Transient Analysis of Multifluid Interaction with Structure," Los Alamos National Laboratory report (to be published).

TRAC INDEPENDENT ASSESSMENT  
FIN A7053

INTRODUCTION (T. D. Knight)

During fiscal year 1982 the Transient Reactor Analysis Code (TRAC) independent assessment program is working both on TRAC-PD2 and TRAC-PF1. The TRAC-PD2 work concentrates on large-break loss-of-coolant (LOCA) analyses. We have started all of the TRAC-PD2 related subtasks. The TRAC-PF1 work involves the analyses of tests related to small-break LOCA and non-LOCA transients.

TRAC-PD2 ANALYSIS OF SEMISCALE TEST S-07-6 (C. P. Booker)

Semiscale Mod-3 test S-07-6 exhibited long period oscillations during reflood and remains an unresolved analysis problem.<sup>1</sup> This test simulated a 200% double-ended offset-shear break. Downcomer heat-transfer effects have been hypothesized as the cause of the reflood oscillations. We have modified the TRAC-PD2 vessel component to include the multiple-material, one-dimensional heat-conduction structures from TRAC-PF1. This additional detail in the wall-conduction solution for the vessel and downcomer regions is necessary to model the complex heat-transfer processes. The input decks are complete and are being adjusted to provide the correct steady-state and boundary conditions.

TRAC-PD2 ANALYSES FOR BATTELLE COLUMBUS LABORATORY DOWNCOMER TESTS  
(J. K. Meier)

The TRAC-PD2 code has produced flooding curves corresponding to three experimentally derived flooding curves from the Battelle Columbus Laboratory (BCL) 2/15-scale steam-water plenum-filling tests. These curves are characterized by high inlet liquid flow with low subcooling (case 1), high inlet liquid flow with high subcooling (case 2), and low inlet liquid flow with high subcooling (case 3). The flooding curves were produced by varying the steam flow. TRAC predicted well the flooding curve for case 1, with the calculated steam flow at complete bypass ~10% lower than the data show. However, for cases 2 and 3 the steam flow was 30% to 35% lower than in the data. The impact of this underprediction on pressurized-water-reactor analyses



is obscured because the steam flow varies rapidly during the time bypass occurs.

#### TRAC-PF1 ANALYSIS OF SEMISCALE TEST S-UT-7 (B. E. Boyack)

Semiscale Mod-2A test S-UT-7 simulated a 5% communicative cold-leg break with upper-head injection. The preliminary TRAC-PF1 calculation compares well with the test data in most respects. The code calculated both the timing and magnitude of phenomena occurring in the intact and broken loops; also, the calculated break flow compared favorably with the data. However, the calculated core liquid inventory was low and resulted in an unrealistic core dryout. Parametric studies are in progress to investigate the dryout.

#### REFERENCES

1. R. J. Mattson, "Status of Semiscale Test S-07-6," Nuclear Regulatory Commission memorandum to O. Bassett (October 27, 1981).

TRAC APPLICATIONS TO 2D/3D  
FIN A7049

INTRODUCTION (K. Williams)

A systematic comparison of the Transient Reactor Analysis Code (TRAC-PD2/MOD1) with the Slab Core Test Facility (SCTF) pressure-effects tests was made this quarter. Good agreement with data and correct prediction of parametric trends, as in the Cylindrical Core Test Facility (CCTF) calculations, were obtained. An independent review of these results by Yukio Sudo, visiting scientist from the Japan Atomic Energy Research Institute (JAERI), corroborated these conclusions and also indicated areas for future code model improvement (particularly entrainment and de-entrainment).

UPPER PLENUM TEST FACILITY (M. Cappiello)

TRAC-PF1 design/evaluation studies have been completed for the German proposed modifications to the Upper Plenum Test Facility (UPTF). This study included evaluation of the possible use of steam injection directly into the steam-water separator to force the emergency core coolant (ECC) into the reactor vessel. Also investigated was a feedback-controlled steam injection system. The final results from this study will be presented to 2D/3D personnel early next quarter. Technical Notes also will be prepared.

SLAB CORE TEST FACILITY (S. Smith and Y. Sudo)

A blind posttest calculation of SCTF Run 506, a high-pressure test, was completed with TRAC-PD2/MOD1 using initial conditions provided by JAERI. The comparison was good between the calculation and the data for rod temperatures, turnaround times, quench envelopes, core differential pressures, mass inventories, and loop velocities. The comparison was not as good for absolute pressures, upper plenum pool formation and fluid temperatures, and mass accumulation in the steam-water separator. Some evident discrepancies can be explained by code anomalies or deficiencies, such as the nonphysical wide-band

pressure surges experienced during the calculation, the omission of radiation between rods and walls, the irregular liquid entrainment from the core to the upper plenum, and the lack of a de-entrainment model specifically for the upper plenum. In general, however, the recently revised calculational model and TRAC-PD2/MOD1 give good agreement with the test data.

A blind posttest calculation of SCTF Run 507, the base-case test, was completed with TRAC-PD2/MOD1. The Run 507 calculation compared well with the data for rod temperatures, turnaround times, quench envelopes, core differential pressures, mass inventories, and loop velocities. The comparison was fair for absolute pressures, upper plenum pool formation, fluid temperatures, and mass accumulation in the steam-water separator. Figure 1 compares SCTF Test 507 heater rod surface temperatures and the TRAC-PD2 predictions at six axial elevations in Bundle 2. The predicted rod surface temperature histories are in good agreement with the experiment at all axial elevations. Similar agreement was obtained in the other bundles.

A blind posttest calculation of SCTF Run 508, the low-pressure test, was also completed with TRAC-PD2/MOD1. The calculation and the data compared well for core differential pressures, pressure-vessel mass inventories, pressure-vessel absolute pressures, temperature turnaround times, and temperature histories in lower core elevations. The comparison was fair for upper plenum pool formation, fluid temperatures, mass accumulation in the steam-water separator, rod temperatures and turnaround times, and quench envelopes in higher core elevations.

The TRAC and the SCTF results have been compared by Y. Sudo of JAERI for these forced-flooding, system pressure-effects tests (Runs 506, 507, and 508). The results show that the TRAC can predict well the overall transients of core rod temperatures (see Fig. 2), core differential pressure, and liquid carryover into the hot leg, as well as in the upper plenum -- effects that are strongly dependent on the system pressure. However, these comparisons also show differences between the SCTF test and the TRAC results that should be improved in the future.

CYLINDRICAL CORE TEST FACILITY (R. Fujita, F. Motley, and T. Okubo)

Both the coarse-node and the fine-node input models for CCTF have been converted to the TRAC-PF1 format. Analysis of the Core-I base case (Run 14) is in progress. Preliminary results indicate that the core-to-downcomer oscillations that were calculated with TRAC-PD2 at bottom-of-core recovery (BOCREC) are still a problem with TRAC-PF1.

2D/3D PROGRAM TECHNICAL NOTES

"TRAC Analysis of the SCTF High Pressure Shakedown Test (Run 506)," Suzanne T. Smith (LA-2D/3D-TN-81-22).

"TRAC Analysis of the SCTF Base Case Test (Run 507)," Suzanne T. Smith (LA-2D/3D-TN-81-23).

"TRAC Analysis of the SCTF Low Pressure Test (508)," Suzanne T. Smith (LA-2D/3D-TN-81-24).

"Analysis of TRAC and SCTF Results for System Pressure Effects Tests Under Forced Flooding (Runs 506, 507, and 508)," Yukio Sudo (LA-2D/3D-TN-81-33).



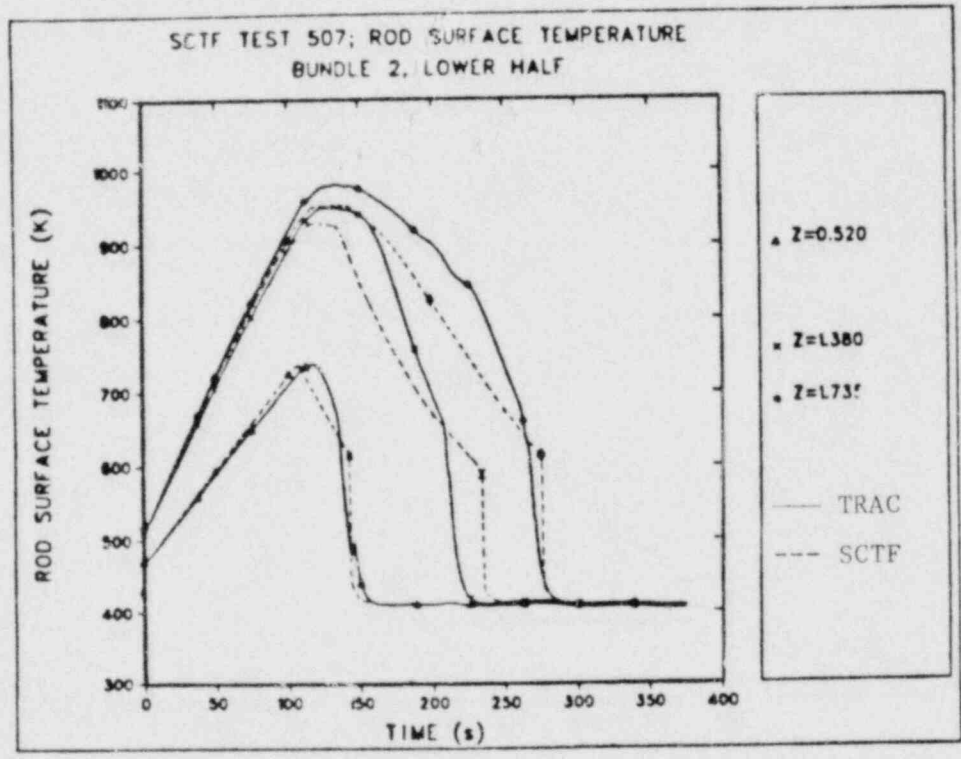
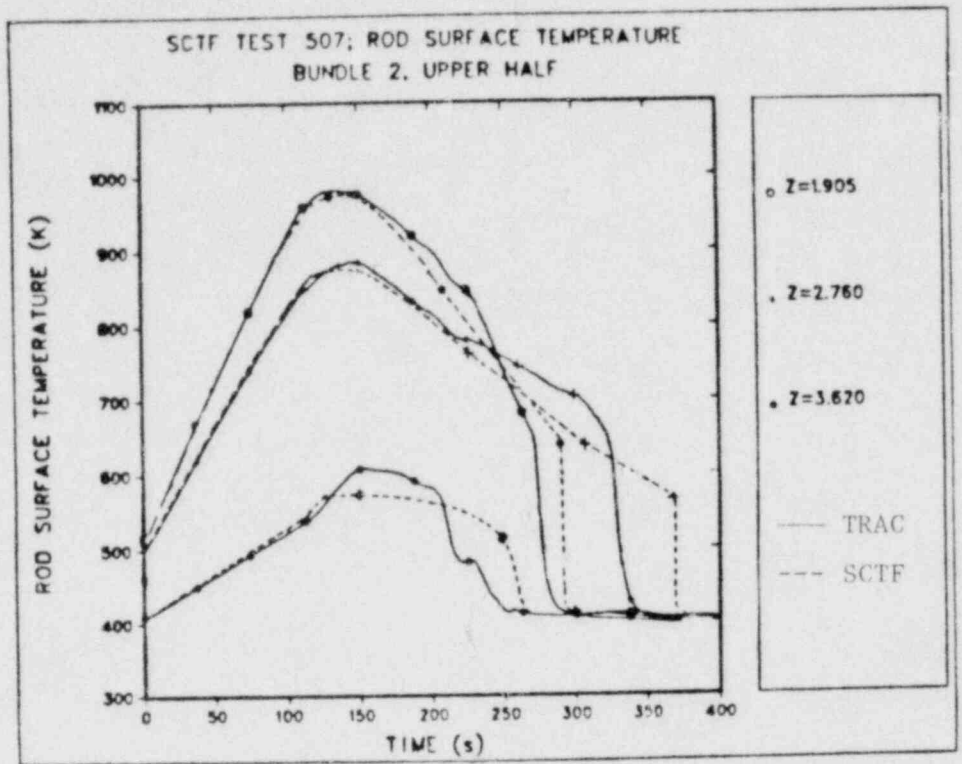


Fig. 1. Comparison between SCTF Test 507 heater rod surface temperatures and TRAC-PD2 predictions at six axial elevations in Bundle 2.

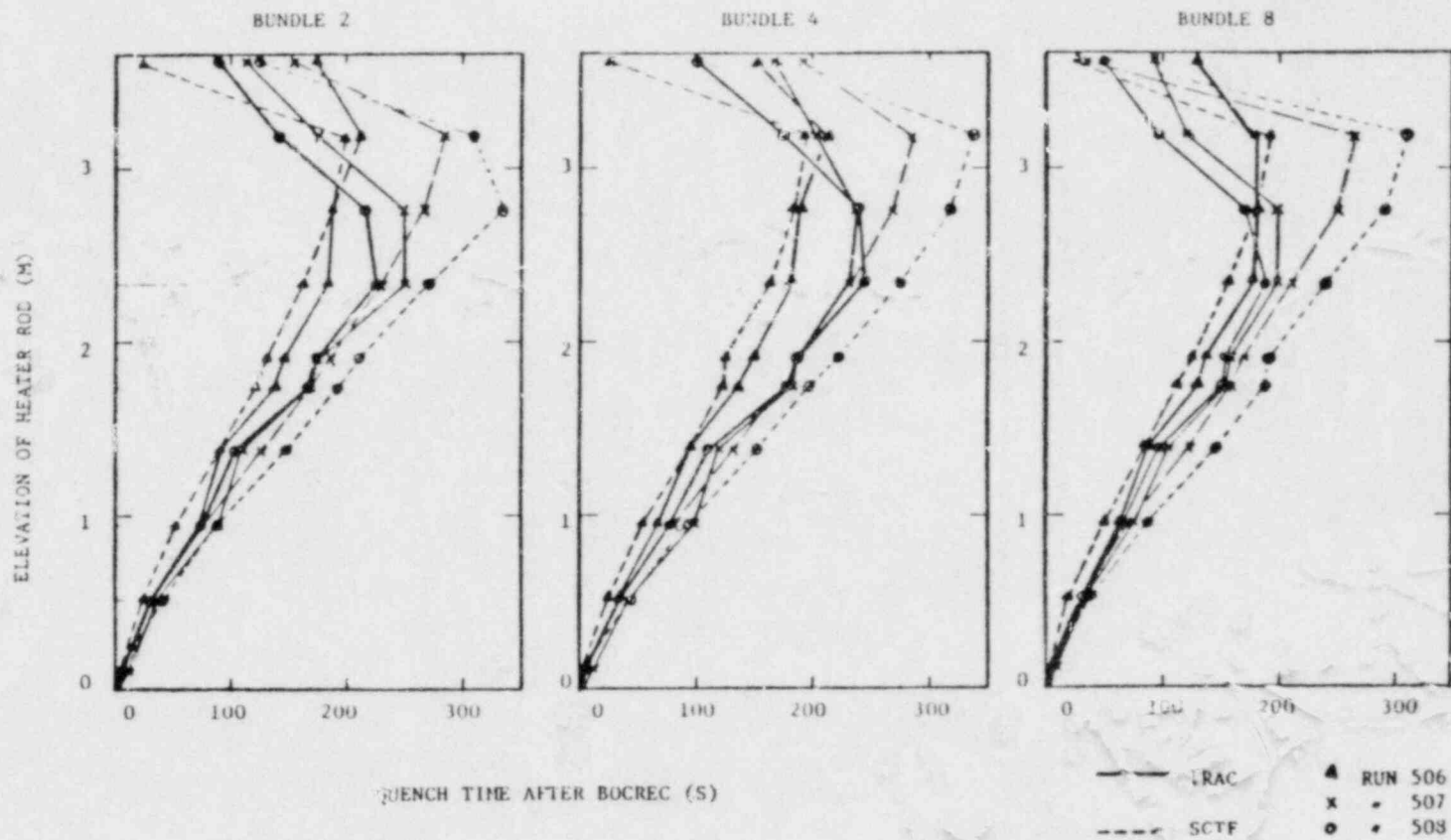


Fig. 2. Comparison of TRAC predicted and measured quench envelopes as a function of core radial position for the SCTF pressure-effects tests.

## METHODS FOR SAFETY ANALYSIS

FIN A7015

### INTRODUCTION (J. E. Wing)

The objective of this work is to develop, apply, and assess methods and models for the analysis of core-disruptive accidents. This work provides effective accident analysis tools to the Nuclear Regulatory Commission (NRC) for the assessment of the consequences of core-disruptive accidents in either liquid-metal-cooled fast breeder reactors (LMFBRs) or light-water reactors (LWRs). Assistance also is provided to the NRC, Division of Accident Evaluation, to maintain cognizance of the safety design bases of US and foreign advanced reactor concepts and to support such other NRC activities as the development of rules for degraded core cooling.

### TRANSITION-PHASE CALCULATIONS (L. B. Luck)

Transition-phase studies based on the Conceptual Design Study (CDS) Phase-1 reactor have continued and focused on factors affecting axial-blanket blockage formation. These studies were delayed pending the resolution of SAS3D-to-SIMMER-II data translation difficulties, as described in the code improvement section of this report.

Two SIMMER-II transition-phase calculations have been performed using the results of an improved SAS3D initiating-phase calculation. In the first calculation, early control subassembly failure resulted from high temperatures and high liquid velocities in the lead driver region. Because the failure occurred with the control assembly essentially full of liquid sodium, large-scale intermixing and pressurization of the driver region resulted. In this case, ejection of most of the fuel from this driver region eliminated possibility of later recriticality and the calculation was terminated.

Because of the large uncertainty in phenomena modeling for such a sequence, a second calculation was performed where the failure was prevented arbitrarily. In this calculation, no recriticality was predicted; however, the recriticality potential remained high for an extended period. Preliminary

analysis indicated that small-scale fuel-sodium interactions in the lower axial blankets resulted in sufficient sodium streaming through the core regions to keep the liquid fuel in a dispersed, subcritical state.

#### CODE IMPROVEMENT EFFORTS (L. B. Luck)

In early SIMMER-II transition-phase calculations, cladding blockages formed during the initiating phase were treated as steel particles with constrained mobility. Study of the effect of blockages upon core fuel removal and fuel-sodium interactions in the axial blankets, however, required a structure representation of frozen relocated cladding. Modifications both to SASSIM and to SIMMER-II accomplished this change. Other problems resolved include the treatment of differences between the SAS3D and SIMMER-II axial mesh and the effects of inconsistencies between the SAS3D and SIMMER-II pressure calculations where multicomponent effects are significant. Because of the increasing complexity and size of SASSIM, a stand-alone version of the code was created.

Nuclear cross-section processing is required both for SAS3D and for SIMMER-II. The processing treatments used should be consistent in cases where the accident calculation is transferred from SAS3D to SIMMER-II. To ensure consistency and to minimize the potential for errors in procedure, a new processing code has been developed to perform the separate functions of energy group collapse, cross-section shielding, and file mode conversions.

#### SIMMER CODE DEVELOPMENT (V. Martinez)

The new SIMMER postprocessor, T6POST, is now about 90% complete and testing of its various options has started. A Control Data 7600 version has been made available to users who are willing to help test it. Versions for other computers have yet to be written.

In addition to the combined capabilities of its two predecessors, T6POST and NEUTRONICS, T6POST has the following capabilities.



- (1) An interactive graphics display may be selected.
- (2) Comparison plots may be made between problems or between variables at selected times.
- (3) It can rotate three-dimensional plots on either a vertical or horizontal axis.
- (4) It will postprocess up to three problems in the same run.
- (5) It can create new variables from existing ones for plotting.
- (6) Any number of variables may be selected from a given group for postprocessing.
- (7) The number of equally spaced curves to be used for contour plotting may be selected.
- (8) Five different types of integration plots are available.
- (9) It will automatically select two- or three-dimensional plots for cell trace plotting.
- (10) Restarting capabilities are available.
- (11) It will accept special plotting routines.

#### ADVANCED METHODS FOR LMFBR SAFETY ANALYSIS (W. R. Bohl)

We applied the new SIMMER-II pressure iteration algorithm to model a vapor explosion. The event sequence consisted of three steps: (a) coarse mixing with film boiling, (b) a triggering event followed by fine fragmentation and propagation leading to efficient liquid-liquid heat transfer, and (c) expansion of the reaction products.

This event sequence required that significant constitutive relationship model changes be made, including radiation energy transfer in film boiling and nonequilibrium vaporization-condensation. The results were compared to vapor-explosion tests performed by Sandia National Laboratories in a thermite and water system. Some qualitative agreement was obtained, although problems remain regarding appropriate physical assumptions. Extrapolation to fast-reactor materials demonstrated the importance of the working-fluid thermal diffusivity.

#### REFERENCES:

1. M. G. Stevenson, Compiler, "Nuclear Reactor Safety, April 1 - June 30, 1981," Los Alamos National Laboratory report LA-9209-PR, NUREG/CR-2281, Vol. 2.

ADVANCED CONVERTER SAFETY RESEARCH  
FIN A7014

STRUCTURAL INVESTIGATION TASK (C. A. Anderson)

In the structural analysis of Prestressed Concrete Reinforced Vessels (PCRVs) we are running the NONSAP-C code on a posttensioned concrete containment shell with a large reinforced penetration. This is a large problem with a large stiffness matrix ( $\sim 2 \times 10^6$  entries) and a matrix bandwidth of  $\sim 2000$ . Analyses of the problem using NONSAP-C on the CRAY computer gave unacceptable running times caused, we believe, by disk reads and writes. We have modified NONSAP-C to minimize the disk input/output (I/O), which we hope will reduce running time on the CRAY. Also, we are evaluating a concrete cracking model based on the theoretical work of Budiansky and O'Connell<sup>1</sup> that predicts concrete stiffness as a function of crack density. Model predictions are being compared with experimental data on concrete inelastic behavior under conditions of uniform uniaxial, biaxial, and triaxial stress.

We are developing graphite failure criteria that account both for primary and secondary (thermal) stress effects as well as the observed wide scatter in tensile and compressive strength of graphite test specimens. For ductile metals, less emphasis is given to secondary stresses in failure criteria according to American Society of Mechanical Engineers (ASME) code rules. However, because of the brittle nature of graphite, it is not clear that primary and secondary stresses shouldn't be added directly and used in failure criteria. This issue is of considerable importance to the field of High-Temperature Gas-Cooled Reactors (HTGRs) because large graphite structural components (for example, the core support block) are subjected both to primary and to significant secondary stresses during operation and under certain accident conditions. After a review of work done at General Atomic Inc., Oak Ridge National Laboratory, and the Franklin Institute on graphite failure criteria, we are developing a program plan to identify new graphite failure criteria that reflect

- the brittle nature of graphite,
- the statistical nature of graphite properties, and
- the presence of secondary (thermal) stresses.

#### SYSTEMS ANALYSIS TASK (K. R. Stroh)

The Fort St. Vrain (FSV) model in the Composite HTGR Analysis Program, Version 2 (CHAP-2) was executed with maximum coded detail on the Digital Equipment Corporation (DEC) VAX 11/780 computer. The CHAP-2 code modeled the entire nuclear-steam-supply, balance-of-plant, plant-protective, and control systems. The model included a 37-channel core model, with 1 channel for each FSV refueling region and with 8 axial nodes corresponding to the top reflector, the 6 active core regions, and the bottom reflector/core-support structure. For this application the Los Alamos Systems Analysis Code, Version 2 (LASAN-2), numerically solved a system of 804 ordinary differential equations (ODEs) and 65 implicit algebraic equations, a total of 869 state variables. This exercise encountered no code problems and verified that LASAN-2 can handle very large systems of ODEs. However, CHAP-2 did execute very slowly, primarily because of the finite-difference Jacobian calculation.

Los Alamos provided preliminary copies of the LASAN-2 code to Brookhaven National Laboratory and Oak Ridge National Laboratory; we will address their comments in the released code. Also, we transmitted LASAN-2 to the General Electric Company, Sunnyvale, California, for use in the process-heat Very High-Temperature Reactor (VHTR) Systems Code (STAR), funded by the Department of Energy.

The documentation of CHAP-2 and LASAN-2 is progressing.

#### REFERENCES

1. B. Budiansky and R. J. O'Connell, "Elastic Moduli of the Cracked Solids," *Int'l J. Solids and Structures* 12, 81-97 (1976).

TRAC CALCULATIONAL ASSISTANCE AND USER LIAISON  
FIN A7212

INTRODUCTION (N. S. DeMuth)

In this program we apply the Transient Reactor Analysis Code (TRAC) to a variety of transients and postulated accident scenarios for answers to important light-water-reactor (LWR) safety issues. These applications include quick-response calculations, more detailed analyses for safety issues such as the effects of terminating reactor coolant pump operation during small-break loss-of-coolant accidents (SBLOCAs), and eventual application of TRAC to anticipated transients without scram (ATWS) and boiling-water-reactor (BWR) transients. Other work includes liaison with outside users of TRAC to assist them in applying the code to problems of interest.

EFFECTS OF THE REACTOR COOLANT PUMPS ON A SMALL-BREAK LOSS-OF-COOLANT ACCIDENT  
(Jan L. Elliott)

The optimum mode of pump operation during a SBLOCA became an important issue as a result of the accident at Three Mile Island. It is believed that tripping the last two (of four) reactor coolant pumps during the accident led to core damage. A series of calculations modeling a SBLOCA in a Westinghouse pressurized water reactor (PWR) has been performed to aid in determining whether it is preferable to trip the pumps at high-pressure injection (HPI) initiation (the present operator directive), at some later time in the transient, or whether it is preferable to leave the pumps running indefinitely.

Many of the major events in the pumps on/off calculations are similar. The break, located downstream of the pump between the emergency core coolant (ECC) injection point and the vessel, initiated the transient at time zero. The system rapidly depressurized, reaching saturation conditions at 7.7 MPa. The reactor tripped on a low-pressure signal in the pressurizer (13.16 MPa) at 10.1 s. Automatic safety systems isolated the secondary side of the steam generator by tripping the main feedwater and by closing the main-steam-line valve. High-pressure injection also began at this time. The auxiliary feedwater flow was initiated 60 s after the reactor trip signal, allowing time

for the diesel generators to start. Full ECC injection was modeled with the initial accumulator pressure at 4.24 MPa and the low-pressure injection (LPI) setpoint at 1.07 MPa. Temperatures remained well below the steady-state values in all the accident sequences.

Primary system mass (Fig. 1) differed significantly for the pumps-off and pumps-on cases. For the pumps-off case, the loop seals were plugged from 200 to 500 s, which resulted in a high-density fluid exiting the break. This accounted for the major difference initially between system mass for the pumps-off and pumps-on cases. The next major difference was the large quantity of accumulator liquid lost through the break when the pumps were not running. The operating pumps maintained a two-phase mixture of uniform void fraction throughout the system, allowing it to refill substantially; if the pumps were not operating, the fluid drained out the break.

For the delayed-pump-trip cases, the primary effect of tripping the pumps was phase separation leading to the drainage of liquid to the lower elevations of the system. The core, which was partially voided, filled almost completely in seconds. Thus, the delayed pump trip resulted in less core uncover than the pumps-on case, but because the system refilled as slowly as for the pumps-off-at-HP<sub>1</sub>-initiation case (See Fig. 1), the optimum mode of operation was to leave the pumps running indefinitely.

In conclusion, for a 4-in.-diam cold-leg break, the mode of pump operation does not make a significant difference in terms of fuel rod temperatures. With respect to system mass loss, loop seal behavior has important effects, and the calculations for Westinghouse plants show the preferable mode of pump operation is to leave the pumps running.

#### MAIN-STEAM-LINE-BREAK (MSLB) TRANSIENTS FOR THE OCONEE-1 REACTOR

(D. E. Lamkin)

Two TRAC-PD2 calculations were performed to predict the primary-coolant-system pressure and temperature transients that would result from a postulated MSLB with runaway feedwater in the Oconee I plant. These calculations were motivated by Nuclear Regulatory Commission concerns regarding the "pressurized thermal shock" problem for reactor vessels. In particular, a



comparison was desired with calculations for a similar transient performed by Brookhaven National Laboratory with the IRT code, a PWR system transient code.<sup>1</sup>

Both TRAC calculations assumed instantaneous rupture of a single 34-in.-i.d. main steam line at time zero. The calculations differed in the modeling of the pressurizer and also incorporated somewhat different assumptions regarding the feedwater flow to the broken steam generator.

Case 1: Feedwater flow continued for 15 min after MSLB at a flow rate of  $1.138 \text{ m}^3/\text{s}$ . Feedwater temperature was held at 553 K for 40.0 s, then decreased linearly to 305.5 K over the next 2 min. The pressurizer was modeled with the conventional PRIZER module in TRAC using four nodes.

Case 2: Feedwater flow continued for 15 min after MSLB at a flow rate of 886 kg/s for 15 min. (This is somewhat greater than the flow rate in Case 1.) The feedwater temperature history is the same as in Case 1. The pressurizer was modeled with a PIPE module using 20 nodes.

The rapid blowdown of the secondary coolant system following the MSLB, and later the flashing of the continuing feedwater, produced substantial overcooling and depressurization of the primary system. Figures 2 and 3, respectively, show our computed primary-coolant pressure and cold-leg-coolant temperature histories. For comparison, the corresponding results from the IRT calculations<sup>1</sup> are plotted on the same graphs. The coolant temperatures calculated by TRAC and IRT agree well. However, TRAC predicts a higher minimum pressure and lesser pressure recovery than IRT. Insufficient information is available at present regarding the details of the IRT calculation to offer an explanation of this difference.

TRAC USER LIAISON (C. E. Watson)

The user liaison section had 32 interactions on various problems this quarter. Since TRAC-PF1 had just been released, most problems were

PF1-related. We informed some users of how to correct the air option so it would work in the presence of a completely subcooled liquid-filled cell. This correction was obtained from the code development group. A nozzle problem that had not run successfully with PD2 gave reasonable answers when run with PF1.

The effect of pressurizer noding on primary-system pressures was investigated after the results of two TRAC calculations, a main-steam-line break and a steam-generator overfill transient, exhibited a discontinuous pressure change as each node filled. In both these calculations, the pressurizer was represented as a four-node PRIZER (semi-implicit) component. A test problem was devised in which a time-dependent fill ( $V_{inlet} = 10$  m/s) injected cold liquid into a surge line (PIPE component) connected to the pressurizer. The system pressure was calculated with the pressurizer modeled as a 4-node and 20-node PRIZER (semi-implicit) and as a 20-node (fully implicit) PIPE component. The pressure histories obtained from the 4-node PRIZER and the 20-node PIPE are compared in Fig. 1. The calculated system pressure during refilling of the pressurizer is dependent on the pressurizer model and on the number of nodes. Other calculations with smaller inlet flows exhibit similar behavior although the differences in pressure are smaller. This shows sensitivity of pressure to noding that should be considered in modeling transients with appreciable pressurizer-surge-line fill rates.

A computer program, EXTRACT, was modified for use in restarting calculations with TRAC-PF1, version 7.0. EXTRACT reads data for a specified component from the binary TRAC dump file and writes the data to a new file in a format suitable for input into the code. This permits changes to component data, and the problem can be restarted with the current values of the thermodynamic and flow quantities (such as temperatures, pressures, void fractions, and velocities).

#### REFERENCES

1. R. C. Kryter, R. D. Cheverton, F. B. K. Kam, T. J. Burns, R. A. Hedrick, and C. W. Mayo, "Evaluation of Pressurized Thermal Shock," Oak Ridge National Laboratory report NUREG/CR-2083, ORNL/TM-8072 (October, 1981).

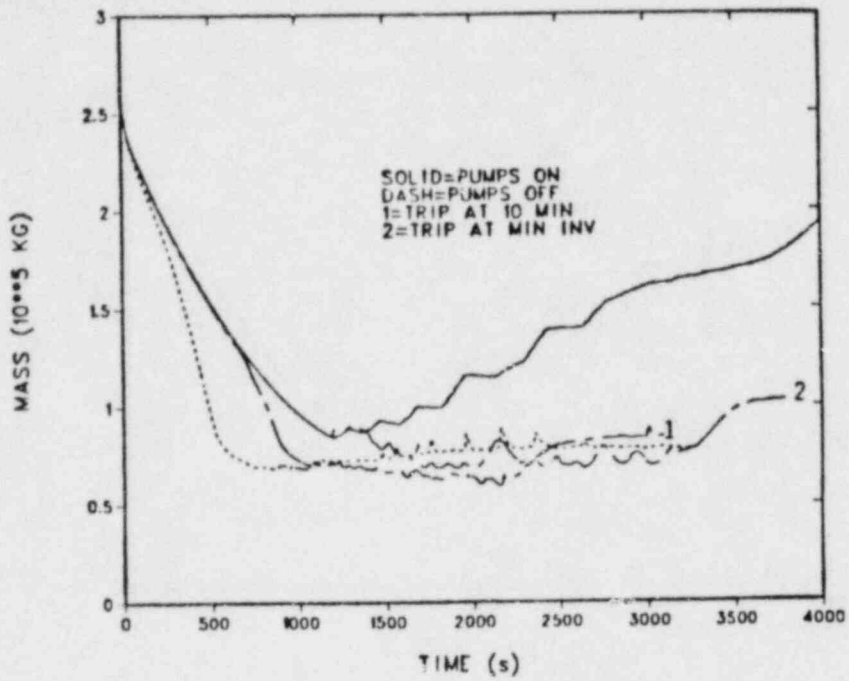


Fig. 1. Primary system masses for four modes of pump operation.

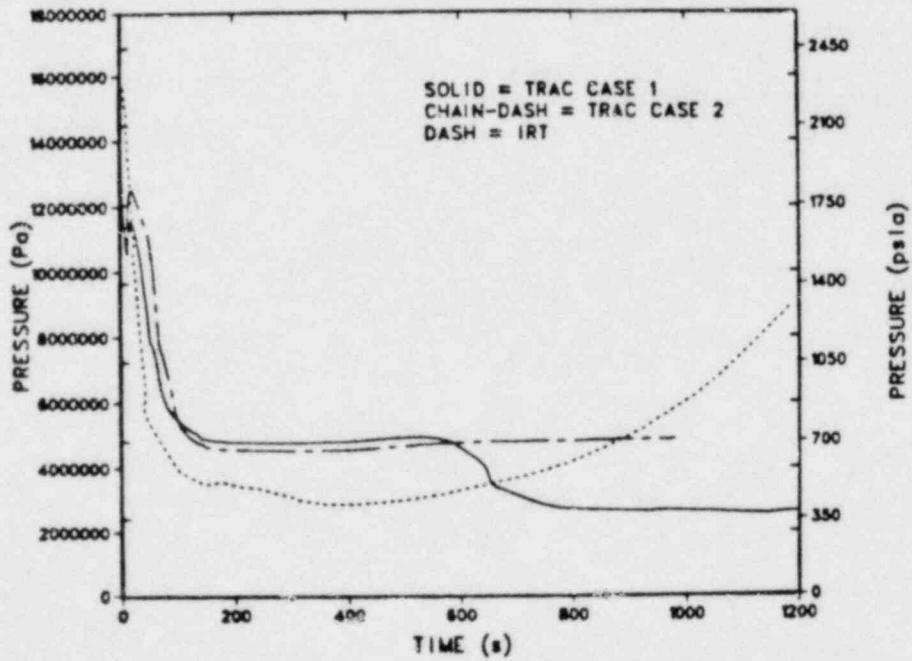


Fig. 2. Primary-coolant system pressure.

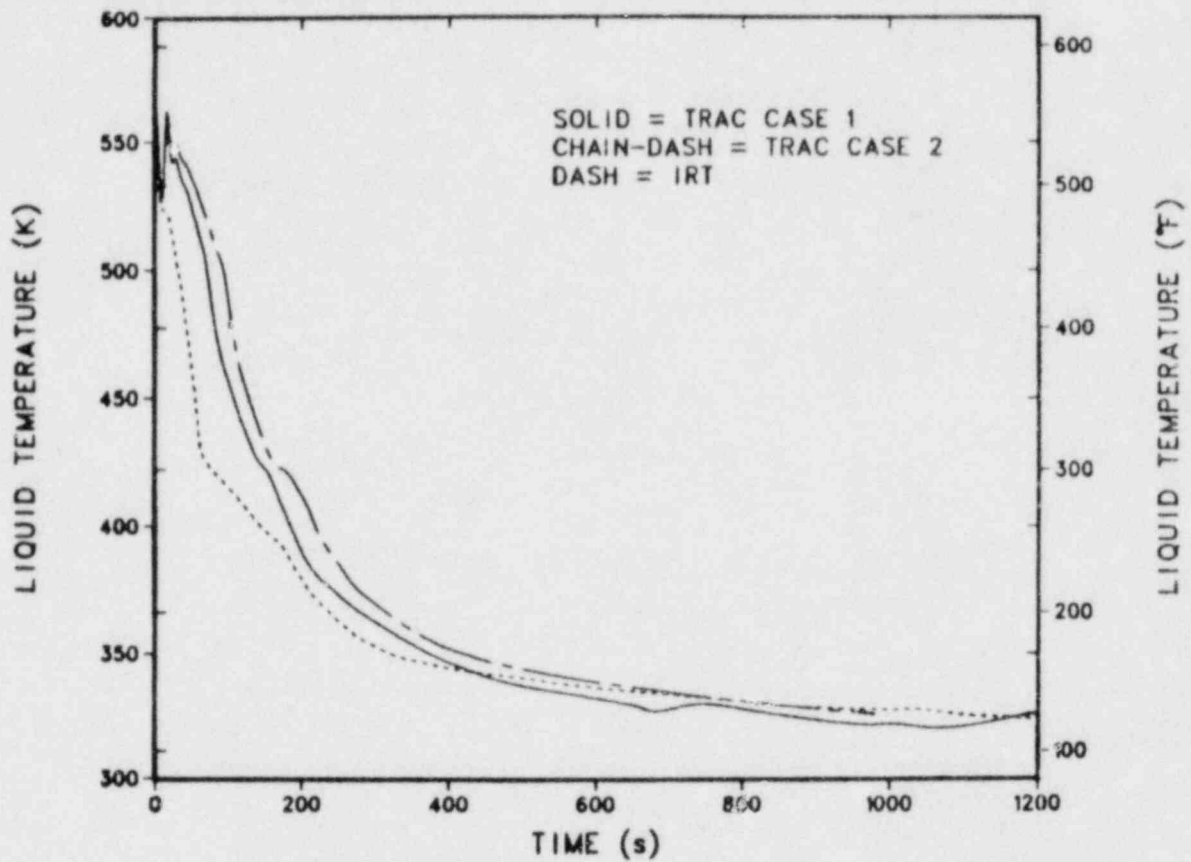


Fig. 3. Primary-coolant cold-leg temperature in the loop with the broken steam line.

SEVERE ACCIDENT SEQUENCE ANALYSIS PROGRAM  
FIN A7228

INTRODUCTION (J. E. Wing)

The objective of Severe Accident Sequence Analysis (SASA) research is to improve light-water-reactor (LWR) safety through further understanding of severe accident phenomena and the man-machine interface during accidents.

UNMITIGATED BORON DILUTION EVENTS (R. J. Henninger)

The consequences of unmitigated boron dilution events in a pressurized water reactor (PWR) have been investigated with TRAC-PF1. When a PWR is shut down for refueling, a high boron concentration in the primary coolant (for example, 1200 ppm by weight for the Zion-1 plant) is necessary to maintain subcriticality. The boron concentration is normally well above that required for subcriticality (for example, 2000 ppm for Zion-1). Inadvertant startup of a pump and an opened valve could lead to the addition of unborated water to the primary system. This, in turn, could lead to dilution of boron in the core, to criticality, and to a subsequent power excursion unless the operator acts to terminate the dilution process.

The analysis was performed using a TRAC-PF1 model of the Zion-1 plant. Calculations assumed that refueling was complete (that is, the core was at a beginning-of-equilibrium-cycle state with all of the control rods inserted). Two configurations of the system were considered. In the first, the vessel was closed and the system was filled to the normal operating level, but the system was still at atmospheric pressure. In the second, the vessel was open and filled to the head flange. If unborated water enters the system at the maximum rate and the volume of the primary coolant being diluted is that of the vessel excluding the upper head, criticality is reached in 75 min. With these assumptions, only the coolant in the vessel has been diluted; the remainder of the primary system is at the original (higher) concentration. TRAC-PF1 calculations started with the reactor at low power (10 kW) and just critical. The positive reactivity associated with continued dilution of the coolant in the reactor vessel was computed and used as input to the calculation. The



resultant power excursion for the closed-vessel case is given in Fig. 1. Feedback from increasing fuel and coolant temperatures limits the peak power to 120 MW. In an auxiliary calculation, feedback from coolant temperature was eliminated. The peak power in that calculation was 20% higher. Thus, the peak power was determined largely by fuel temperature (Doppler) feedback. In the closed-vessel case, heating of the coolant in the core region induced natural circulation in the primary system (See Fig. 2.). This resulted in flow into the core of cooler water with a higher boron concentration. The higher boron concentration terminated the excursion and the flow stopped.

Continued dilution with the vessel closed will result in another excursion within 75 min. Termination of the second excursion would require boiling in the core region and associated negative void reactivity. In view of the indications that will be received in the control room from the first excursion, it appears likely that the operator will intervene and terminate the diluting flow. Therefore, we ended our calculations at this point.

#### PRESSURIZED-THERMAL-SHOCK-INDUCED VESSEL RUPTURES (D. Dobranich)

Vessel ruptures believed to result from repressurization following a severe overcooling transient are being investigated to determine the adequacy of the emergency core coolant (ECC) system to cool the fuel rods. The analyses are being performed for the Oconee-1, Babcock and Wilcox PWR using the reactor analysis code, TRAC-PD2 MOD2.

The initiating event for the overcooling transient was a main-steam-line break (MSLB) with runaway feedwater (full flow for 15 min) on one of the once-through steam generators. Contraction of the primary liquid caused by rapid cooling created voids in the primary system. High-pressure injection (HPI) was initiated on a low-pressure signal and gradually refilled these voids. We assumed no operator action to throttle the HPI after the pressurizer level returned to its normal range, and this led to repressurization of the primary with subsequent vessel rupture. Wall and liquid temperatures ranged from 325 K to 400 K throughout the system at the end of the overcooling transient.

To evaluate the effectiveness of the ECC flow in cooling the core, ruptures in the vessel wall near the core midplane were simulated; calculations were

performed for several break sizes that spanned the range of design-basis events for breaks in cold-leg piping. Calculations for one "small" break ( $1.01 \times 10^{-3} \text{ m}^2$ ) showed that flow from the HPI would equilibrate with the leakage flow to keep the core covered. For another small break ( $4.05 \times 10^{-3} \text{ m}^2$ ), the rupture caused depressurization of the primary to the set point of the low-pressure injection (LPI) system. In this case the combined flow from the HPI and LPI systems equilibrated with the leakage flow to keep the core covered. For a  $1.0 \times 10^{-2} \text{ m}^2$  rupture, the combined HPI and LPI flows were still sufficient to prevent core uncovering. The rupture flow, along with the total LPI and HPI flow, is shown in Fig. 3 for this case.

A rupture equivalent to a double-ended cold-leg break ( $0.794 \text{ m}^2$ ) at the core midplane then was assumed to be an upper bound for determining the ability of the ECC to prevent core damage. Because the primary liquid was far subcooled at the time of vessel rupture, little vaporization occurred in the system during blowdown. About 18000 kg of water (16%) remained in the vessel at the end of blowdown. ECC injection, including HPI, accumulator, and LPI, began refilling the vessel almost immediately. Liquid volume fractions in the core and lower plenum are shown in Fig. 4. The vessel filled to the level of the break so the lower half of the core was covered with liquid, while the upper half was filled with steam. Vapor generation in the lower half of the core, however, produced upward steam flows with velocities of about 7-8 m/s. These high velocities persisted throughout the transient because the vent valves in the upper plenum opened and provided a flow path to the downcomer and break. The high steam flow, together with entrained droplets, cooled the uncovered portion of the core.

Further investigation of this cooling, however, led to the discovery of a modeling deficiency in the heat-transfer package. The Biasi correlation, used in TRAC for calculating the critical heat flux temperature (TCHF), overpredicts TCHF at high values of the vapor fraction. TRAC, therefore, determined that heat transfer was in the nucleate boiling regime, which yielded unreasonably high values for the heat-transfer coefficients. The problem was alleviated by limiting TCHF. This modification inhibited nucleate boiling, and the uncovered portion of the core was no longer cooled effectively by the steam flow. Heat transfer was by transition boiling of entrained droplets and forced convection to vapor, so rod temperatures at the top of the core began to rise at about 0.6

K/s. Core damage will begin within 20 min at this rate. Cladding temperatures at the core top, midplane, and bottom are shown in Fig. 5.

Rupture sizes greater than approximately  $3.0 \times 10^{-2} \text{ m}^2$  will result in cladding damage at the upper elevations of the core. For rupture sizes less than  $3.0 \times 10^{-2} \text{ m}^2$ , the HPI and LPI flow will prevent cladding damage as long as recirculation of the emergency injection liquid is maintained.

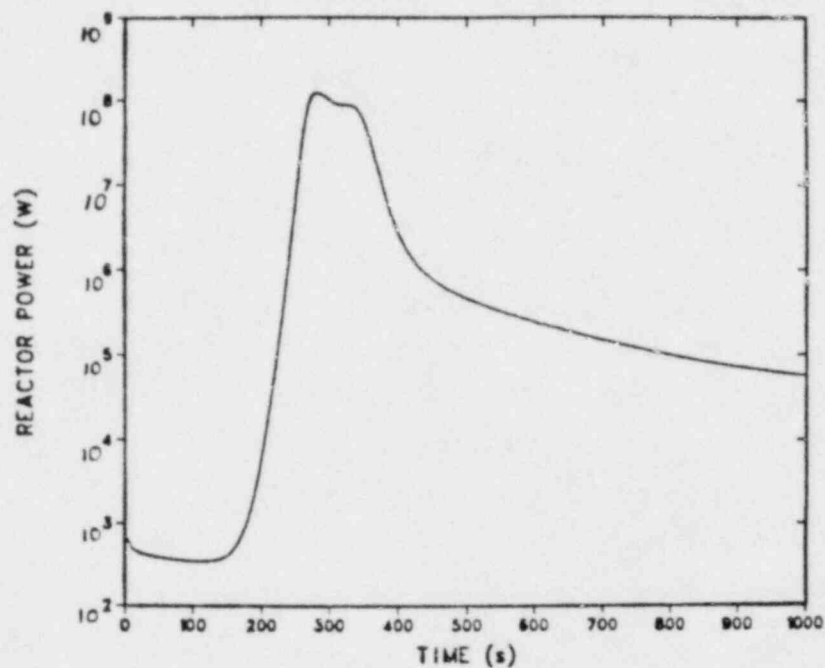


Fig. 1. Reactor power in the closed-vessel case is limited by Doppler and coolant temperature feedback. The excursion then is terminated by the flow of higher boron concentration coolant.

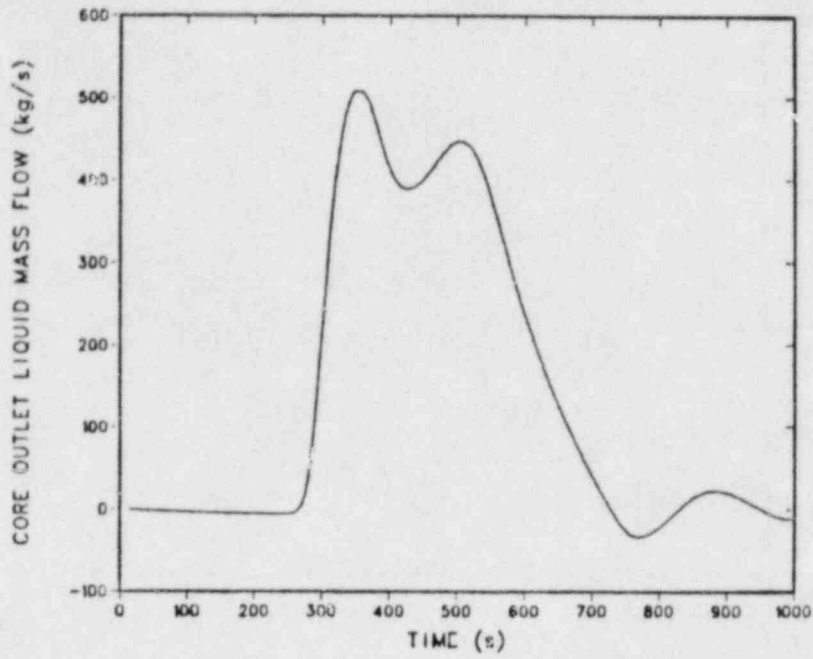


Fig. 2. Coolant flow is induced by elevated temperature in the core region.

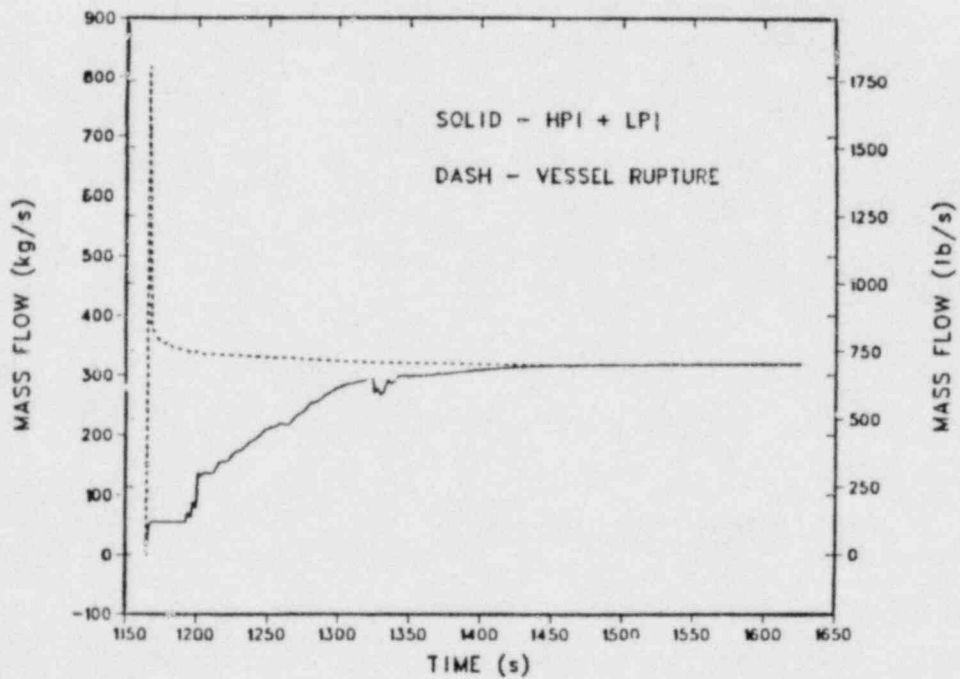


Fig. 3. Flow response for 0.01-m<sup>2</sup> vessel-rupture transient.

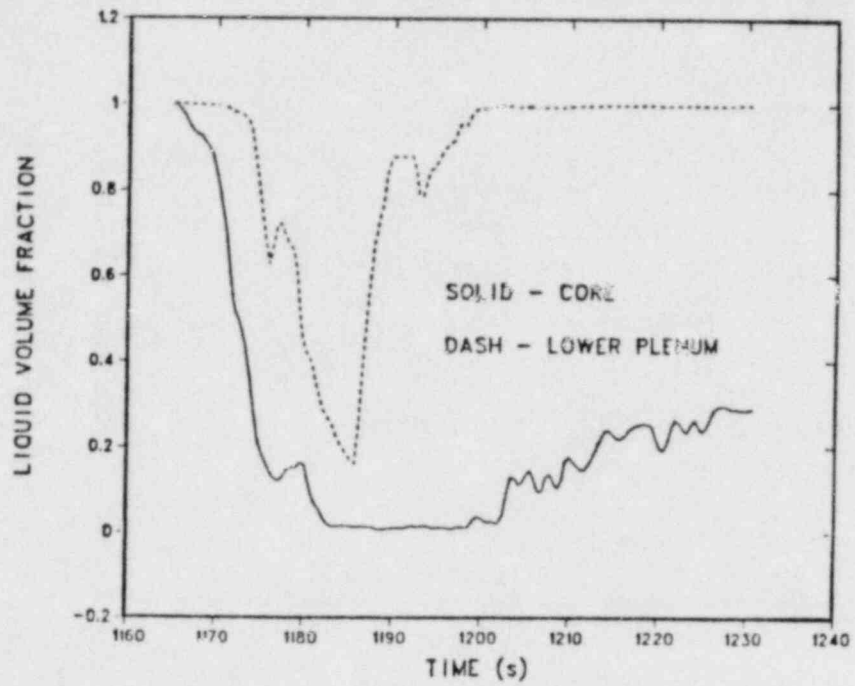


Fig. 4. Refill characteristics for 1.8-m<sup>2</sup> vessel-rupture transient.

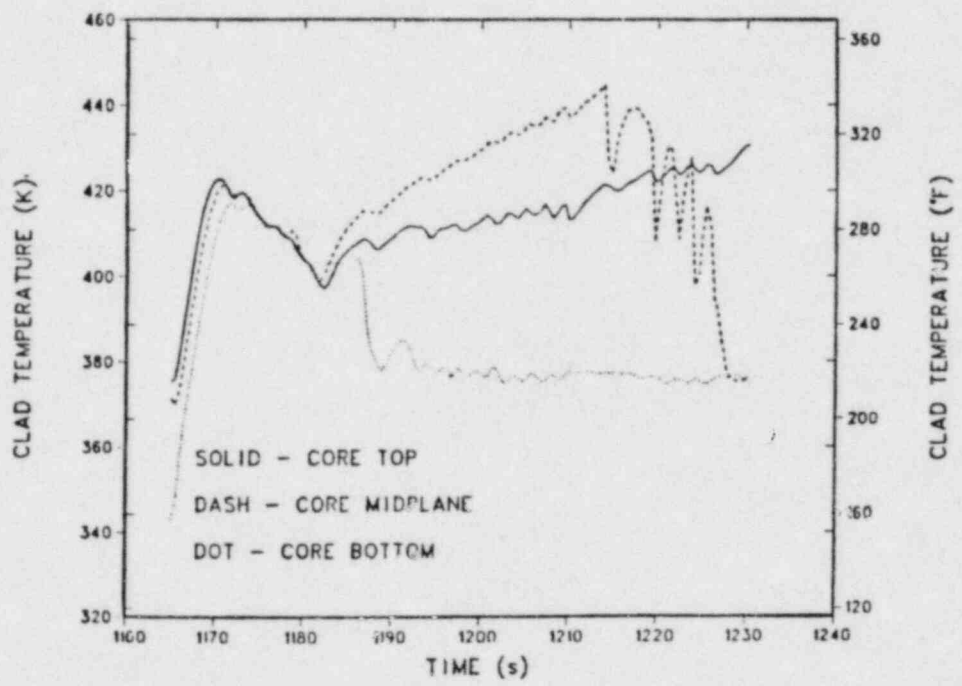


Fig. 5. Temperature response for 1.8-m<sup>2</sup> vessel-rupture transient.



UPPER STRUCTURE DYNAMIC EXPERIMENTS  
Fin A7235

UPPER STRUCTURE DYNAMICS EXPERIMENTS (L. Meyer, KFK)

The Upper Structure Dynamics (USD) experiments have been continued with the test section containing the SNR (German breeder reactor) upper axial blanket pin array and SNR mixing head. The pin bundle (Fig. 1) consists of 169 pins each having a length of 172 mm and a diameter of 2.4 mm with a pitch/diameter (P/D) = 1.317. The pins are held by three honeycomb spacer grids (Fig. 2). Figure 3 shows the mixing head that is downstream of the pin bundle. The test section (Fig. 4) has been equipped with five pressure transducers [Kulite Miniature Metal Diaphragm Pressure Transducers, HEM-375, 1.72 MPa (250 psi) and 0.69 MPa (100 psi) full scale] and three thermocouples (NANMAC Pencil Probe Thermocouple, E-12-2-K, Chromel vs Alumel, 10- $\mu$ s response time). Figure 5 shows a schematic of the USD apparatus and its representation by a one-dimensional noding in the  $S_n$  Implicit Multifield, Multicomponent Eulerian Recriticality (SIMMER) code.

Some modifications of the apparatus had to be made to simulate the SNR conditions and to improve the performance of the experiment. A new piston track, longer (1200 mm), and with a more accurate inner diameter, has been build. The piston weight has been reduced to 0.35 kg for similarity with the SNR sodium pool. To reduce the distance from the flashing source to the pin bundle, the spacer behind the rupture disk was reduced to 8 mm (from 52 mm) and was made of insulating material to minimize heat conduction between the heated core and the test section. A further reduction of the distance between the flashing source and the pins was obtained by using metal inserts in the core. These inserts (not shown in Fig. 5) lift the liquid level up to a distance of 1 cm from the rupture disk and maintain the same propanol mass inventory as before. A certain vapor volume below the rupture disk has to be kept to achieve fast opening and fully opened rupture disk pedals.

Table I lists the geometrical data that are necessary to define the test section in SIMMER. The component fractions ( $\alpha$ ) and the ratios of surface area to total volume were calculated with a node radius of  $r = 2.86$  cm. Table II lists the tests performed with the SNR test section in 1981. The first two

tests were performed under the same conditions as the tests with the Clinch River Breeder Reactor (CRBR) geometry. The SIMMER calculations showed that the transient flow in the upper core structure (UCS) consisted mainly of vapor with only a small liquid volume fraction. This also was seen in the high-speed films taken in some of the CRBR tests. For similarity to the prototypic case, a higher fraction of liquid is desired. Hence, for Tests 3 and 4 the vapor space above the liquid was reduced by filling part of the core with aluminum inserts. The pressure histories (see Figs. 6 and 7) and SIMMER calculations suggest that considerably more liquid was driven through the bundle than before. However, it was not possible to obtain the experimental pressure curves with SIMMER calculations, in spite of some modifications of SIMMER and many parameter variations.

Therefore, a systematic investigation of various experimental parameters was started. For a more precise definition of the initial conditions, some modifications of the experimental setup had to be made. All unheated volumes (such as pressure lines to the pressure gauge and the volume of the gauge itself) had to be reduced or abolished, because condensation of propanol vapor in these volumes led to false initial liquid and vapor volumes. Also, the insulation of the core had to be improved to ensure uniform temperatures. For the same reason a new smaller core has been manufactured, so that the metal inserts are no longer necessary. Tests 5 and 6 are the first of a series in which step-by-step changes of initial conditions will be made. Calculations with SIMMER will be performed in parallel for all experiments.

TABLE I

## GEOMETRIC SPECIFICATIONS

	<u>Length (mm)</u>	<u>Hydraulic Diameter (mm)</u>	<u>Void Volume (cm<sup>3</sup>)</u>	<u><math>\alpha</math> Void</u>	<u><math>\alpha</math> Steel</u>	<u><math>\alpha</math> Aluminum</u>	<u>Ratio of Surface Area to Volume of Aluminum (m<sup>-1</sup>)</u>	<u>Ratio of Surface Area to Volume of Steel (m<sup>-1</sup>)</u>
Core 1	374	41	865	0.90	0.10	-	-	83.2
Lower Space	82	50	186	0.88	-	0.12	60.2	-
Pin Bundle	172	2	114.8	0.26	0.32	0.42	56.6	496.0
Middle Space	12	44	18.3	0.59	-	0.41	56.6	-
Mixing Head	82	9.2	67	0.32	-	0.68	93.5	-
Upper Space	127.3	40	169.7	0.52	-	0.43	50.1	-

TABLE II  
EXPERIMENT MATRIX

<u>Test</u>	<u>Fluid</u>	<u>Liquid Volume at 25°C (cm<sup>3</sup>)</u>	<u>Pressure (MPa)</u>	<u>Core Volume (cm<sup>3</sup>)</u>
1	Propanol	319	1.03	865
2	"	600	1.03	865
3	"	190	1.03	430
4	"	280	1.03	430
5	Helium ( 25°C)	-	1.03	630
6	" (190°C)	-	1.03	630

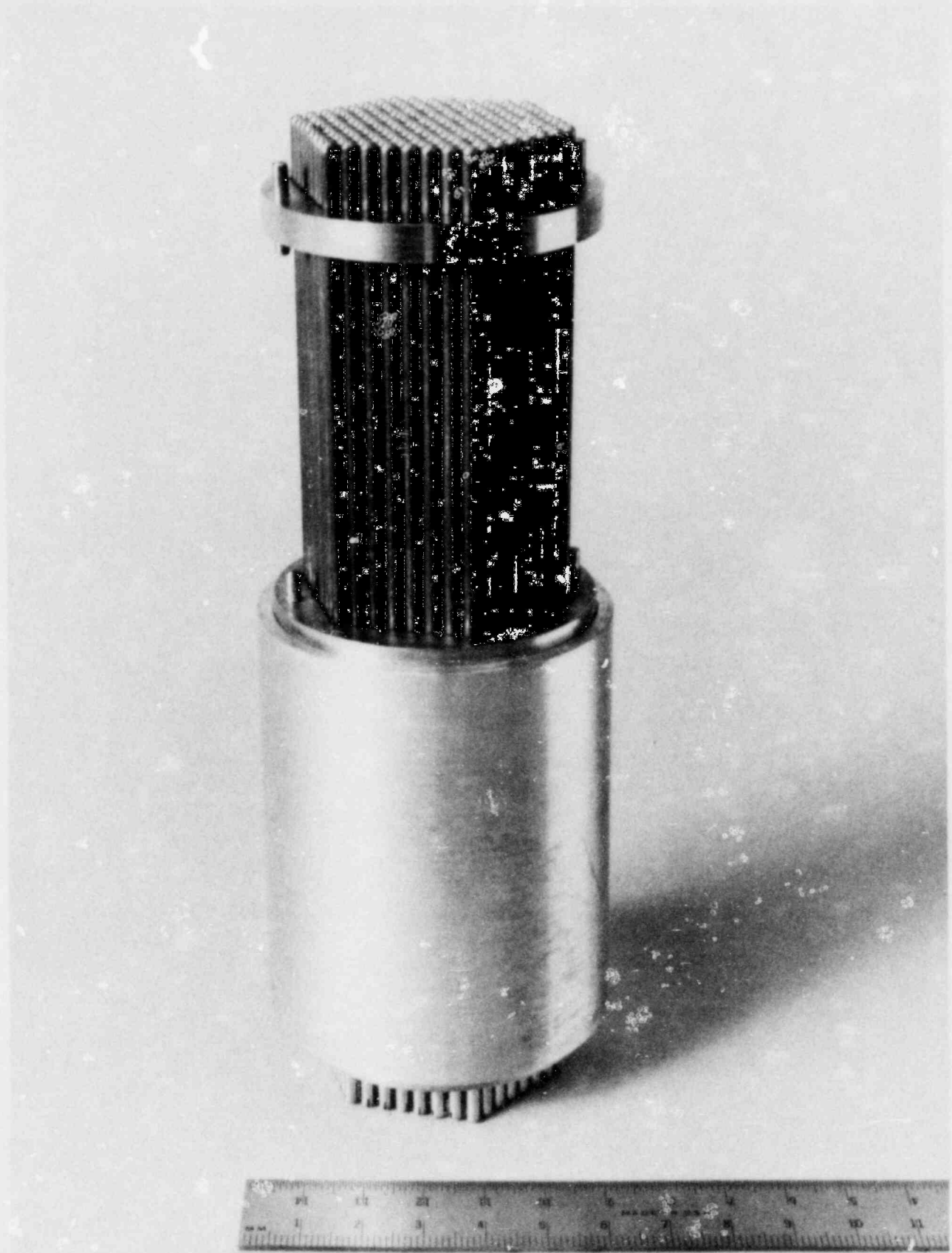


Fig. 1. Pin bundle of the USD-SNR test section.



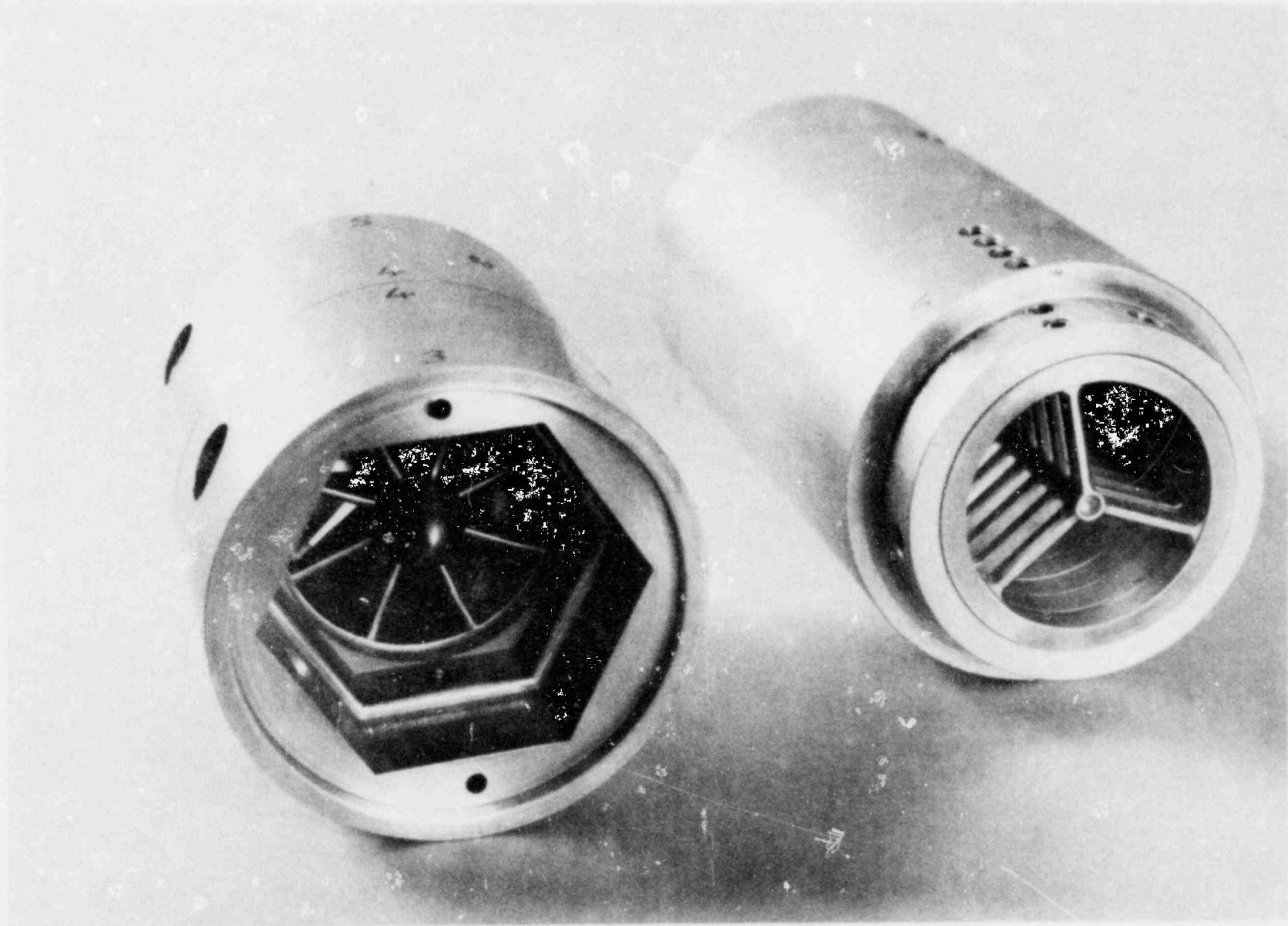


Fig. 2. Spacer grid of the USD-SNR test section.

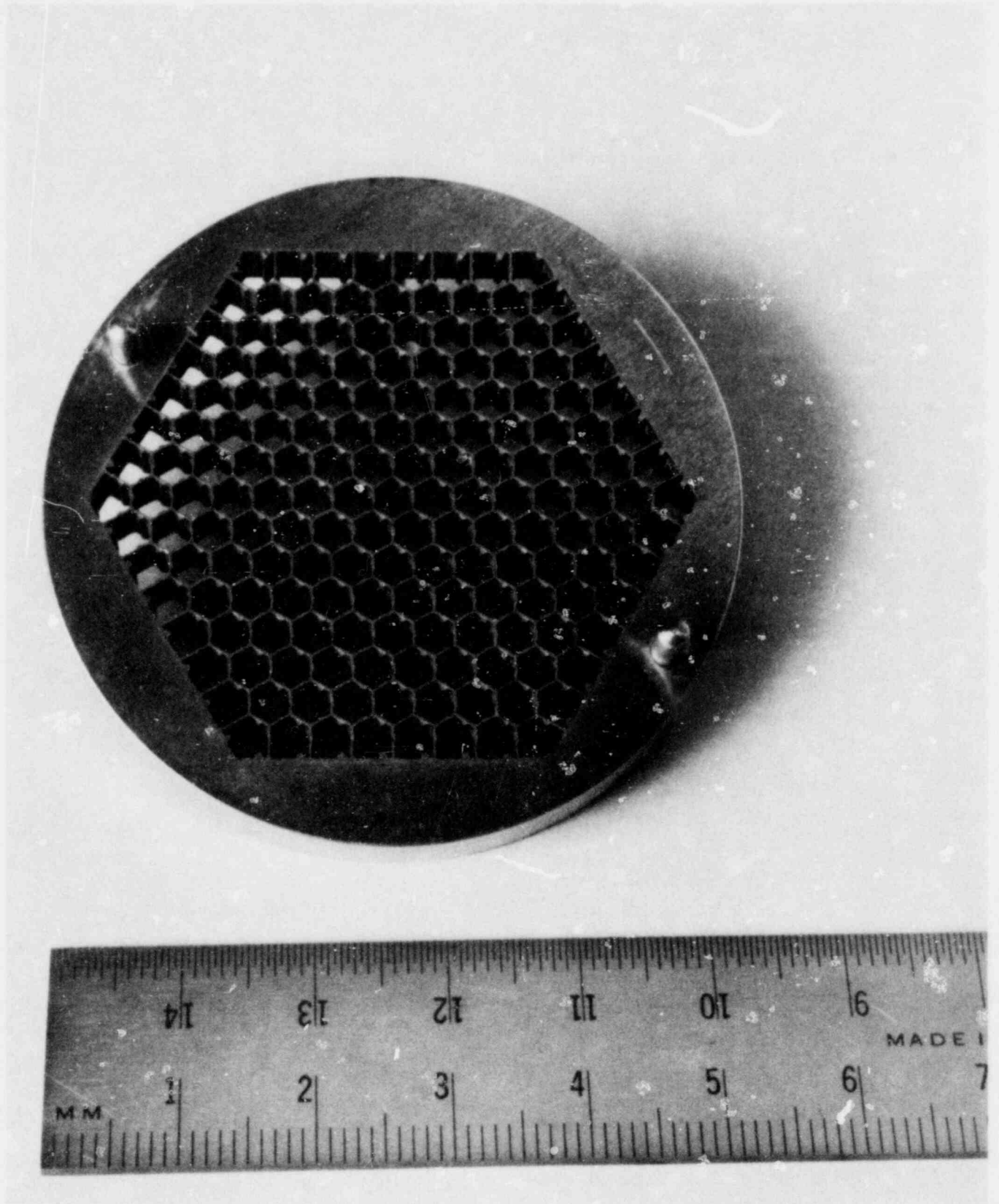


Fig. 3. Mixing head of the USD-SNR test section.

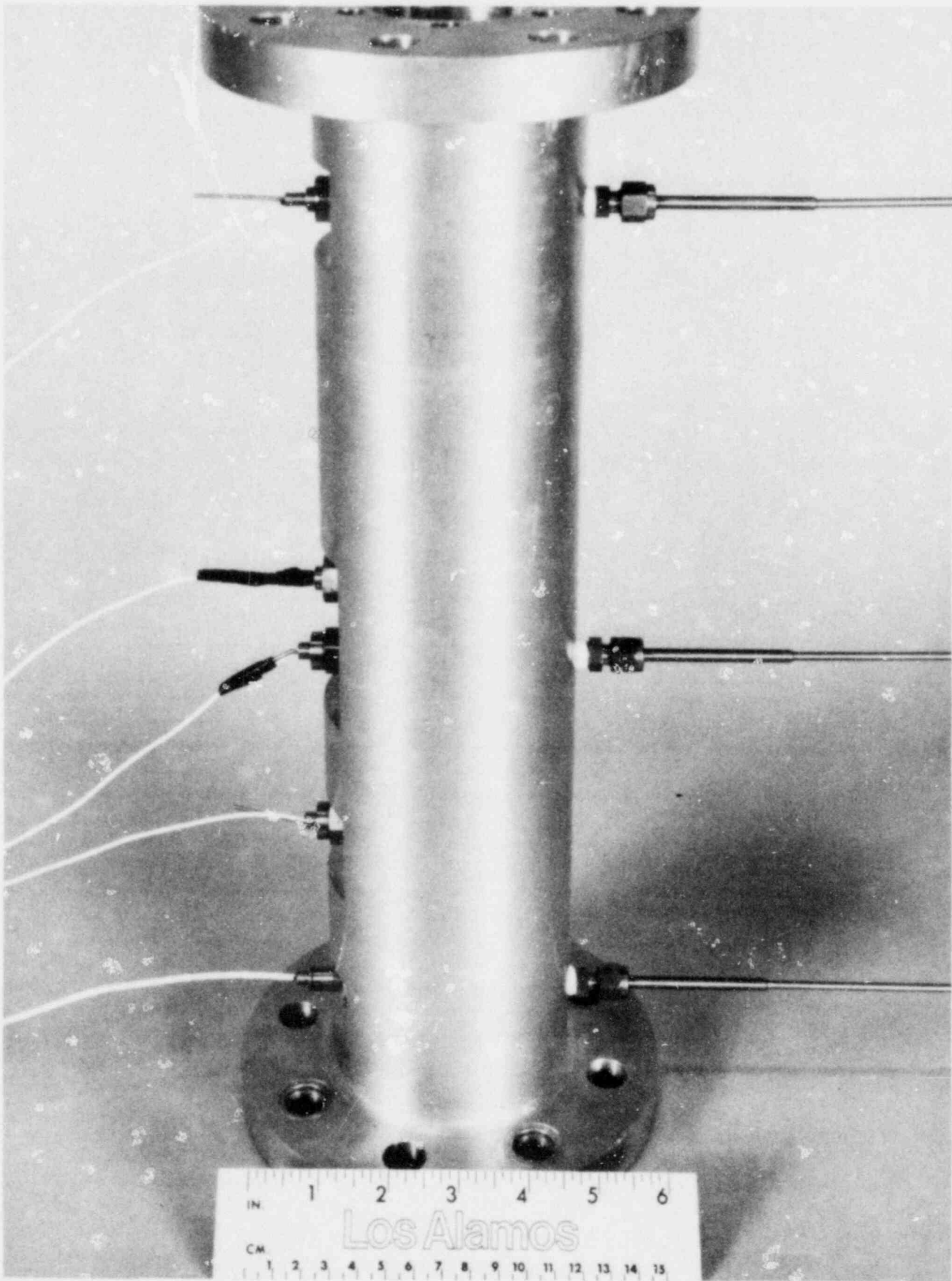


Fig. 4. Instrumentation of the USD-SNR test section.

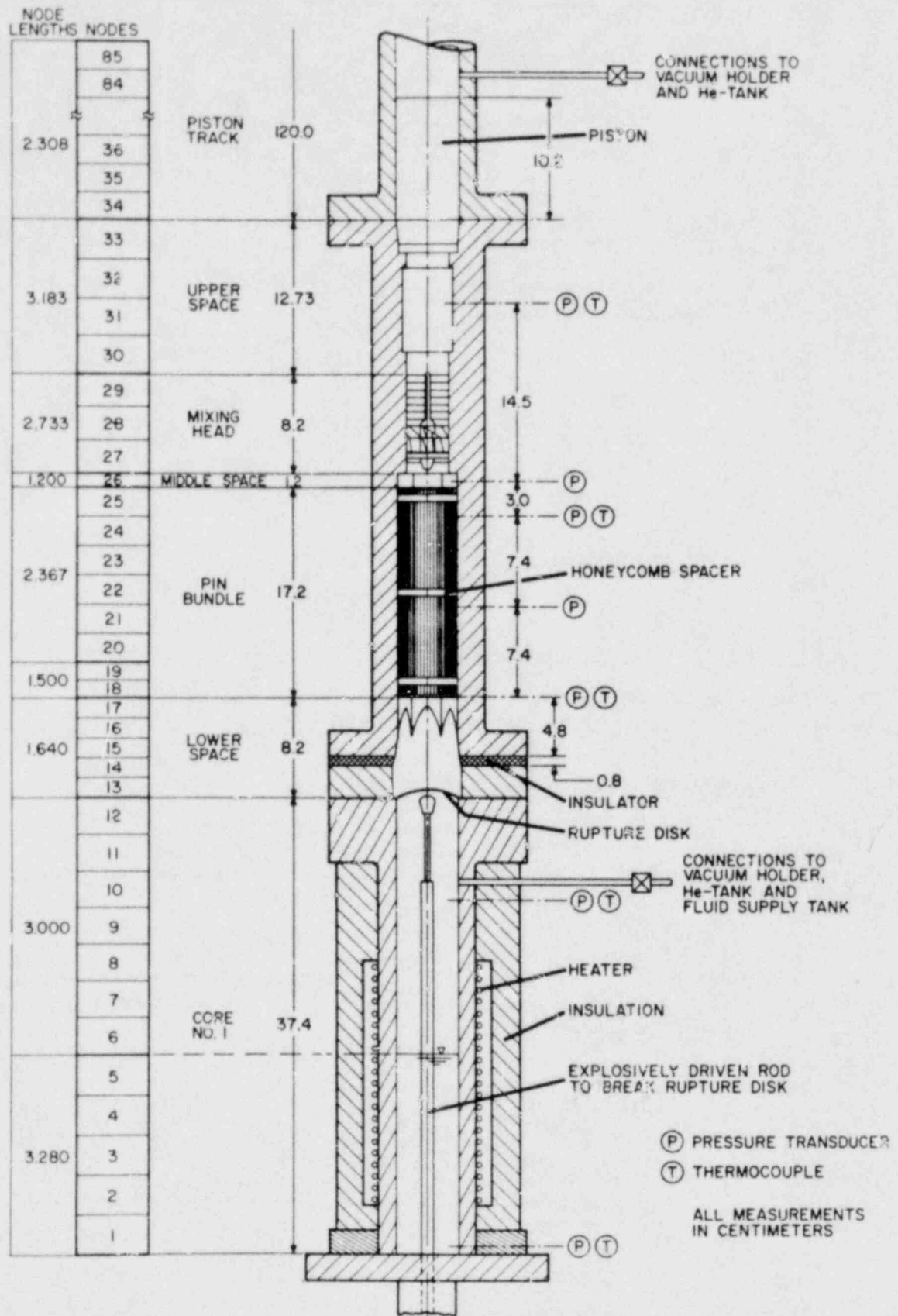


Fig. 5. Schematic of the USD-SNR test apparatus and its representation in SIMMER.

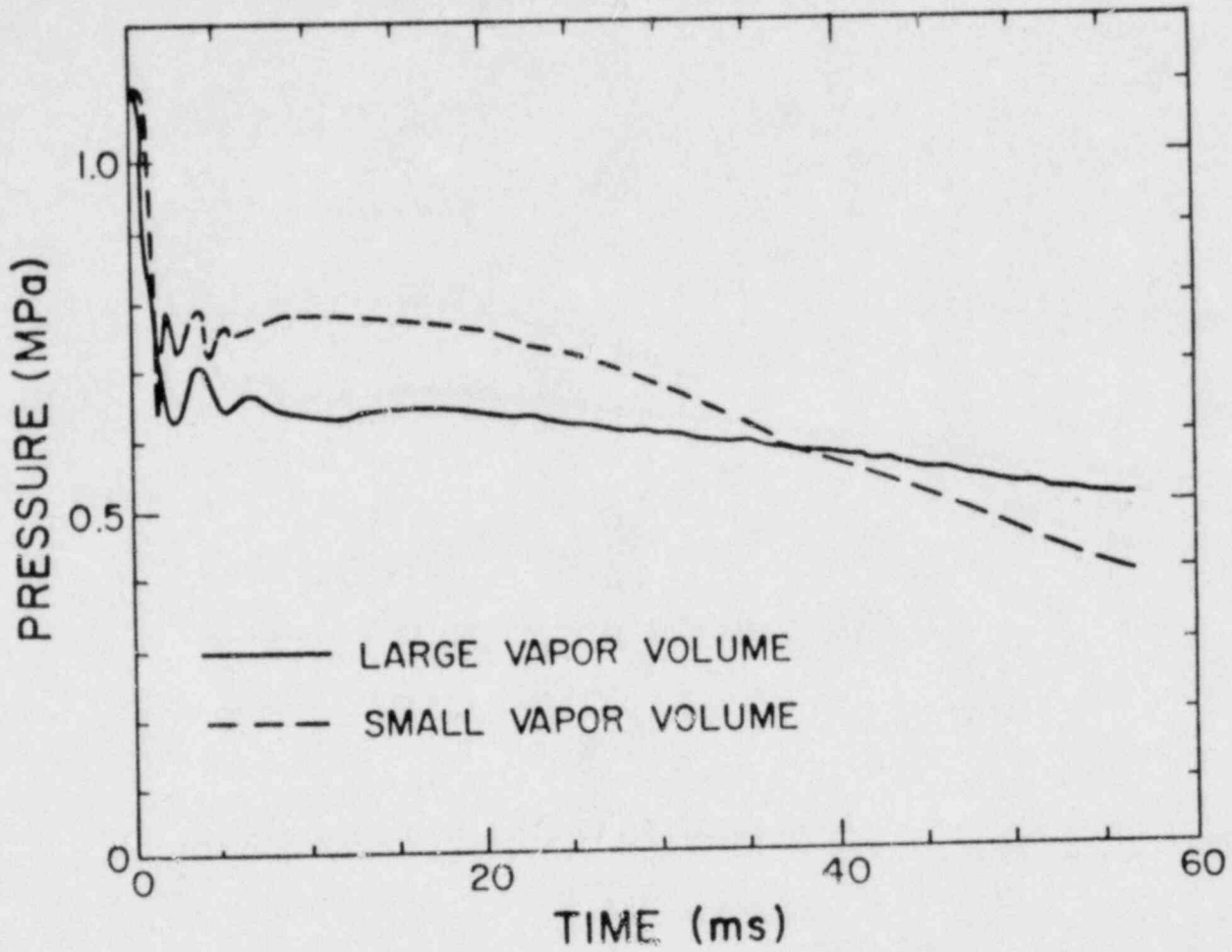


Fig. 6. Core pressure in Tests 1 and 4.

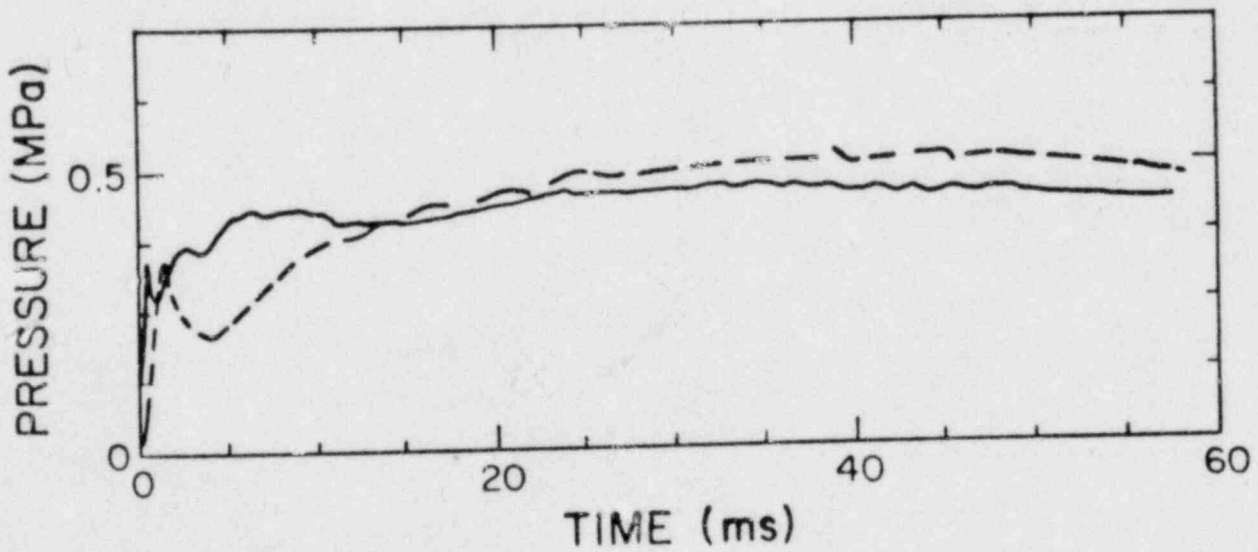


Fig. 7. Pressure in the pin bundle in Tests 1 and 4.



## DISTRIBUTION

	<u>Copies</u>
Nuclear Regulatory Commission, R4, R7, and R8, Bethesda, Maryland	458
Technical Information Center, Oak Ridge, Tennessee	2
Los Alamos National Laboratory, Los Alamos, New Mexico	<u>50</u>
	510

Available from  
GPO Sales Program  
Division of Technical Information and Document Control  
US Nuclear Regulatory Commission  
Washington, DC 20555  
and  
National Technical Information Service  
Springfield, VA 22161